Iranian Journal of Astronomy and Astrophysics
Vol. 9, No. 2, Autumn 2022
©Available online at http://journals.du.ac.ir
DOI:10.22128/ijaa.2022.666.1143

**Iranian Journal of Astronomy and Astrophysics**

# Instability in the Magnetized Accretion Disks with Outflows in the Presence of Self-Gravity

Sekine Karimzade*[1] · Alireza Khesali[2] · Azar Khosravi[3]
[1] Department of Physics, University of Mazandaran, Babolsar, Iran;
*email: karimzade.f@gmail.com
[2] Department of Physics, University of Mazandaran, Babolsar, Iran;
email: khesali@umz.ac.ir
[3] Department of Physics, University of Mazandaran, Babolsar, Iran;
email: a.khosravi@umz.ac.ir

**Abstract**. We study the stability of a model of magnetized accretion disk, in which outflows play a significant role in driving the inflow, and magnetic field is generated by a dynamo operating in the disk. We present a local and linear analysis of the stability in the presence of self-gravity and winds. The numerical results show the model with self-gravity is unstable in all parts, while in a model without self-gravity, instability can be observed only in regions near the central body. Eventually, the effect of wind cooling on the model stability was discussed. According to the results, in systems without self-gravity, wind cooling can help the system towards stability, but in the presence of self-gravity, it is shown that our model will remain unstable in all regions. Comparison of these result with observational evidence shows that this model can be suitable for the explaining the behavior of the disks surrounding young stellar objects.

*Keywords*: Accretion Disks, Outflows, Instability, Magnetic Fields

## 1 Introduction

Now, we know that accretion discs are an integral part of many astrophysical systems, such as active galactic nuclei, binary stars, and young stellar objects, that have been studied for about half a century. It is worth noting that magnetized accretion discs with outflows have been attracting astrophysicists, since with presence of charged particles in disks, magnetic fields play an important role in their structure. Also, outflow that leading to mass loss and consequently, transport angular momentum and energy outward, both can help facilitate the accretion process and affect some of the discs quantities [1-9]. On the other hand, magnetic fields and the outflows are important factors in studying the instability of accretion systems [10-13]. Scientists consider instabilities as the source of many astrophysical processes. Accordingly, since the formation of the theory of accretion discs until today, instabilities in these objects have also been of interest [14-17]. In accretion discs, there can exist many types of instabilities, which take a staple part in the evolution of the discs [18]. For instance, instabilities in accretion systems are the source of turbulence and viscosity [19-20] and many optical fluctuations in discs spectrum can be explained by these instabilities [21-22]. More importantly, by investigating these instabilities, one can find an appropriate explanation for the formation of some parts of the universe, such as the solar system [23-24]. Therefore, the instability problem in magnetized accretion discs with outflow has long been an important topic for study and research.

Lubow et al. (1994, here after LPP94) presented a simple accretion disk model with magnetic winds and considered the stability of such system [25]. In their model, viscosity and self-gravity were neglected and only the effect of the magnetic torque on the accretion process was investigated. Furthermore, they assumed the disc to be vertically isothermal, indeed perturbations in the thermal balance and the disk structure were ignored except for those in the inflow speed. They stated that perturbations of the disk inflow speed were related to perturbations of the wind mass flux, thus the increase in wind mass flux led to increases the inflow speed and the bending of the poloidal magnetic field. Eventually, LPP94 claimed that discs with magnetic winds are intrinsically unstable.

Konigl & Wardle (1996, here after KW96) expressed that the equilibrium model proposed by LPP94 was overly simplified and thus not desirable and the results derived from this model will be unreliable [26]. One of reasons was that LPP94 ignored the effect of gas compression by the disc magnetic field lines at system . However, they used LPP94's method on a more comprehensive model that was proposed by themselves in 1993. KW96 showed that in their model, the mass outflow rate is independent of the inflow speed. They stated that instability of LPP94 does not occur for the magnetized disc with winds in the presence ambipolar diffusion and in general, disc with mass outflow will be immune the most disruptive instability. By implementing numerical simulations, Krasnopolski et al. (1999) attended to the same problem and resulted in the stability of such discs [27].

Campbell (2001) investigated a steady accretion disc model with magnetic winds which the magnetic field is introduced by dynamo mechanism [28]. He showed when perturbations in the disk structure is account for, especially perturbations of magnetic diffusivity $\eta$, the instability proposed by LPP94 will disappear. He demonstrated that perturbations in $\eta$ decreases the bending of the poloidal magnetic field, and in return will prevent from the increase in the inflow speed, thus making his model stable against perturbations.

Cao & Spruit (2002, here after CO02) conducted a linear stability analysis on an approximate equilibrium disk model [29]. Similar to LPP94, they also ignored viscosity in their model. They obtained a dispersion relation in a range of short wavelengths and concluded that if the magnetic torque of the wind is strong enough, the disks with magnetic winds are unstable, and magnetic diffusion in the accretion system stabilizes if the wind torque is small.

Konigl (2004) by conducting another analysis reviewed the model in which KW96 were working [30]. In his analysis, he undermined the results presented by CO02 and expressed that although CO02 had a better physic and solving method than the work done by LPP94, but the extent of the effects of the used approximations on the final results was still unknown. Equilibrium solution curves in Konigl (2004) indicated two stable and unstable branches. He expressed that the developed perturbations in the unstable branch may be the same as the unstable model proposed by LPP94, but the presence of the stable branch means that such discs are not inherently unstable.

Campbell (2009) investigated stability of his previous model more precisely [31]. In works of LPP94 and CO02, viscosity had been ignored, thus they studied case of $N_p \to 0$ that $N_p$ is Magnetic Prandtl number. However, in Campbell (2001), viscosity and magnetic wind torques are comparable, $N_p \sim 1$. In his new work, he considered general values of $N_p$ and researched the thermal balance and vertical equilibrium of the disc. Campbell concluded that such system is unstable.

Li & Begelman (2014) proposed that the outflow can reduce the disk temperature and help to stability. Also, in the presence of outflows, the diffusivity time-scale has been increased and since a amount of the released gravitational energy is transferred to disk outward, $\eta$ will be reduced [12].

Habibi & Abbasi (2019) researched the thermal stability of a thin accretion disc in the presence of a advected magnetic field and winds. They stated that both magnetic pressure and the winds can help with the thermal stability of the system. They could also define a criterion for the disc stability [32].

By reviewing past researches, we conclude that the stability of the magnetized accretion discs with outflows still remain an open problem, which provoked us to search it for a more comprehensive model. In previous work, we considered a magnetized accretion disc model with dynamo mechanism in the presence of wind and self-gravity. One result was that the ratio of viscosity torque to magnetic torque is more than anticipated criterion for the stability of the system [33]. Therefore, in this article, we decided to study stability of this model.

The structure of this paper is as follows. Section 2 involves the basic equations and assumptions governing the model. In Section 3, we investigate the stability of the system. The effect of wind cooling on the model stability is presented in Section 4. Finally, discussion and summary are given in Section 5.

## 2 Basic assumption and equations of the model

A geometrically thin, axisymmetric is studied surrounding a compact accretor of mass $M$ and radius $R$. Cylindrical coordinates $(r, \phi, z)$ are utilized, with the origin at accretor center. The semi-thickness of the disk is marked by $H(r)$ and the disk surfaces are at $z = \pm H(r)$. It is supposed that the disc has a dipole-symmetry magnetic field, so it would be able to emanate magnetically channelled winds from the disk surfaces. Also, we took into account full self-gravity in the model. Therefore, gravitational potential of system, in addition to the central object mass, includes mass of the disk. Following Shakura & Sunyaev (1973), turbulent viscosity $\nu$ is chosen as $\nu = \epsilon c_s H$, where $\epsilon$ is introduced as the rms turbulent Mach number and $c_s$ is the isothermal sound speed [34].
Components of the radial, azimuthal and vertical of momentum equation can be written as

$$\rho(\frac{\partial \upsilon_r}{\partial t} + \upsilon_r(\frac{\partial \upsilon_r}{\partial r}) + \upsilon_z\frac{\partial \upsilon_r}{\partial z} - \frac{\upsilon_\phi^2}{r}) = -\rho\frac{\partial \psi_T}{\partial r} - \frac{\partial P}{\partial r} - \frac{1}{r^2\rho}\frac{\partial}{\partial r}(\frac{r^2B_\phi^2}{2\mu_0}) + B_zJ_\phi, \tag{1}$$

$$\begin{aligned}\rho(\frac{\partial}{\partial t}(r^2\Omega) + \upsilon_r\frac{\partial}{\partial r}(r^2\Omega) + \upsilon_z\frac{\partial}{\partial z}(r^2\Omega)) =& \frac{1}{r}\frac{\partial}{\partial r}(\rho\nu r^3\frac{\partial \Omega}{\partial r}) + \frac{1}{r}\frac{\partial}{\partial r}(\frac{1}{\mu_0}r^2B_rB_\phi) \\ &+ \frac{r}{\mu_0}\frac{\partial}{\partial z}(B_\phi B_z),\end{aligned}$$

$$\rho(\frac{\partial \upsilon_z}{\partial t} + \frac{\partial}{\partial z}(\frac{\upsilon_z^2}{2}) + \upsilon_r\frac{\partial \upsilon_z}{\partial r}) = -\frac{\partial P}{\partial z} - \rho\frac{\partial \psi_T}{\partial z} - \frac{\partial}{\partial z}(\frac{B_\phi^2 + B_r^2}{2\mu_0}) + \frac{1}{\mu_0}B_r\frac{\partial B_z}{\partial r}, \tag{2}$$

where $\Omega = \upsilon_\phi/r$ and $J_\phi = \frac{1}{\mu_0}(\frac{\partial B_r}{\partial z} - \frac{\partial B_z}{\partial r})$ is toroidal current density. Total gravitational potential is given by $\psi_T = \psi_M + \psi_{disk}$. The continuity equation is

$$\frac{\partial \rho}{\partial t} + \frac{\partial}{\partial r}(r\rho\upsilon_r) + \frac{\partial}{\partial z}(r\rho\upsilon_z) = 0. \tag{3}$$

In this model, the source of magnetic fields is a self-sustaining dynamo. Accretion disk dynamos are of an $\alpha\omega - nature$, the interaction of turbulent motions leads to the production of poloidal field from toroidal field that this is named"$\alpha - effect$" and toroidal field is generated from poloidal field by the strong radial shear that is introduced as "$\omega - effect$". By approximations, for a thin disk equation polidal and toroidal components of general mean-field induction equation as follow [35],

$$-\frac{\partial B_z}{\partial t} - \frac{\partial B_r}{\partial t} + \upsilon_rB_z + \eta\frac{\partial B_r}{\partial z} - \alpha B_\phi = 0, \tag{4}$$

$$-\frac{\partial B_\phi}{\partial t}+\eta\frac{\partial^2 B_\phi}{\partial z^2}=-r\Omega' B_r, \tag{5}$$

where $\eta$ is the magnetic diffusivity, it can be related to turbulent viscosity by $N_p=\nu/\eta$, which in our model, is supposed $N_p\sim 1$ [33]. Also, $\alpha$ is the production function of poloidal field and the prime denotes differentiation.

Although, it assumed that the gas pressure in the system is dominant but in the presence of the perturbation we used the general form of the state equation as follow

$$P=P_{gas}+P_{rad}=\frac{\Re}{\mu}\rho T+\frac{1}{3}aT^4. \tag{6}$$

The energy equation for this model is

$$\frac{1}{\Gamma_3-1}[(\frac{\partial}{\partial t}+\upsilon_r\frac{\partial}{\partial r}+\upsilon_z\frac{\partial}{\partial z})P-\Gamma_1\frac{P}{\rho}(\frac{\partial}{\partial t}+\upsilon_r\frac{\partial}{\partial r}+\upsilon_z\frac{\partial}{\partial z})\rho]=\rho\nu(r\frac{\partial\Omega}{\partial r})^2$$
$$+\frac{\eta}{\mu_0}[(\frac{\partial B_\phi}{\partial z})^2+(\frac{\partial B_r}{\partial z}-\frac{\partial B_z}{\partial r})^2+(\frac{1}{r}\frac{\partial}{\partial r}(rB_r))^2]+\frac{1}{r}\frac{\partial}{\partial r}(rK\frac{\partial T}{\partial r})+\frac{\partial}{\partial z}(K\frac{\partial T}{\partial z}), \tag{7}$$

where $K=4\sigma_B/3\kappa\rho$ is the conductivity, $\sigma_B$ and $\kappa$ are the Stefan-Boltzmann constant and the Rosseland mean opacity, respectively. Also, in gas-pressure-dominated case we have $\Gamma_3=\Gamma_1$ and their value is equal to the ratio of specific heats.

$\nabla\cdot\mathbf{B}=0$ in Cylindrical coordinates can be written as

$$\frac{1}{r}\frac{\partial}{\partial r}(rB_r)+\frac{\partial B_z}{\partial z}=0. \tag{8}$$

Poisson equation is given by

$$\frac{1}{r}\frac{\partial}{\partial r}(r\psi_T)+\frac{\partial^2\psi_T}{\partial z^2}=4\pi G\rho \tag{9}$$

# 3 Stability analysis

We use linear and local perturbation method to investigate the system instability [36]. Local analysis means that the perturbation wavelengths must be much shorter than the disc radius, $\lambda\ll r$. Also, by using linear analysis, we can neglect second and higher-order perturbations. After writing basic equations, we proceed as follows

1. The equilibrium state of the system is first defined and then disturbed.
2. System variables should be written as equilibrium variables + perturbation variables.
3. Perturbation state variables should be written exponentially, i.e. $e^{i(k.\vec{r}-\omega t)}$.
4. These variables must be considered in basic equations.
5. In the end, a dispersion relation $k$ must be obtained in terms of $\omega$, and based on its negative or positive, imaginary or real sign, the stability or instability of the system must be determined.

Variables of the system that are subject to perturbations are pressure $P$, density $\rho$, temperature $T$, gravitational potential $\psi_T$, angular velocity $\Omega$, radial velocity $\upsilon_r$, vertical velocity $\upsilon_z$, magnetic field radial component $B_r$, magnetic field azimuthal component $B_\phi$ and the magnetic field vertical component $B_z$. As we have mentioned, these variables are equal to the equilibrium state + the perturbation section. So, we have

$$\begin{aligned}&P = P_0 + P_1, \quad \rho = \rho_0 + \rho_1, \quad \psi_T = \psi_{T0} + \psi_{T1}, \quad T = T_0 + T_1, \quad \Omega = \Omega_0 + \Omega_1,\\ &\upsilon_r = \upsilon_{r0} + \upsilon_{r1}, \quad \upsilon_z = \upsilon_{z0} + \upsilon_{z1}, \quad B_r = B_{r0} + B_{r1}, \quad B_\phi = B_{\phi 0} + B_{\phi 1}, \quad B_z = B_{z0} + B_{z1},\end{aligned} \tag{10}$$

where indexes 0 and 1 refer to the equilibrium state and the perturbation section, respectively. Since we intend to investigate the perturbation in both vertical and radial axes, we consider the perturbation section to be exponential $e^{i(k_r.r+k_z.z-\omega t)}$, where $k_r$ and $k_z$ are radial and vertical components of the wave number, respectively. Then, we add these quantities to the basic equations of the disc, and eventually, the perturbation equations will be obtained. In order to numerically solve, we have made all the obtained perturbation equations dimensionless. Dimensional form of perturbation equations are as follow,

- The continuity equation

$$(\widetilde{\upsilon}_{r0} + i\widetilde{k}_r\widetilde{\upsilon}_{r0} + i\widetilde{k}_z\widetilde{\upsilon}_{z0} - i\widetilde{\omega})\widetilde{\rho}_1 + (1 + i\widetilde{k}_r)\widetilde{\upsilon}_{r1} + i\widetilde{k}_z\widetilde{\upsilon}_{z1} = 0. \tag{11}$$

- The component of the radial of momentum equation

$$\begin{aligned}&(i\widetilde{k}_r\widetilde{\upsilon}_{r0} + i\widetilde{k}_z\widetilde{\upsilon}_{z0} - i\widetilde{\omega})\widetilde{\upsilon}_{r1} - 2\widetilde{\Omega}_0\widetilde{\Omega}_1 - \widetilde{\Omega}_0^2\widetilde{\rho}_1 + i\widetilde{k}_r\widetilde{m}^2\widetilde{P}_1 + i\widetilde{k}_r F\widetilde{\psi}_{T1}\\ &- (i\widetilde{k}_r f_2\widetilde{\upsilon}_A^2 + 2f_2\widetilde{\upsilon}_A^2)\widetilde{B}_{\phi 1} - (i\widetilde{k}_z f_3\widetilde{\upsilon}_A^2)\widetilde{B}_{r1} + (i\widetilde{k}_r f_3\widetilde{\upsilon}_A^2)\widetilde{B}_{z1} = 0.\end{aligned} \tag{12}$$

- The component of the azimuthal of momentum equation

$$\begin{aligned}&(2\widetilde{\Omega}_0 - \frac{\gamma n}{2} - \frac{3}{2})\widetilde{\upsilon}_{r1} + (2\widetilde{\upsilon}_{r0} + i\widetilde{k}_r\widetilde{\upsilon}_{r0} + i\widetilde{k}_z\widetilde{\upsilon}_{z0} - 3i\widetilde{k}_r\widetilde{D}\widetilde{m}\epsilon + \widetilde{D}\widetilde{m}\epsilon\widetilde{k}_r^2 - i\widetilde{\omega})\widetilde{\Omega}_1\\ &+ \frac{1}{4}(8\widetilde{\upsilon}_{r0}\widetilde{\Omega}_0 - 6\widetilde{\upsilon}_{r0} - 2\gamma n\widetilde{\upsilon}_{r0} - 27\widetilde{D}\widetilde{m}\epsilon - 3\widetilde{D}\widetilde{m}\epsilon\gamma n + 6i\widetilde{D}\widetilde{m}\epsilon\widetilde{k}_r + 2i\widetilde{D}\widetilde{m}\epsilon\gamma n\widetilde{k}_r)\widetilde{\rho}_1\\ &- (2f_1\widetilde{\upsilon}_A^2 + i\widetilde{k}_r f_1\widetilde{\upsilon}_A^2 + i\widetilde{k}_z f_3\widetilde{\upsilon}_A^2)\widetilde{B}_{\phi 1} - (2f_2\widetilde{\upsilon}_A^2 + i\widetilde{k}_r f_2\widetilde{\upsilon}_A^2)\widetilde{B}_{r1} - (i\widetilde{k}_z f_2\widetilde{\upsilon}_A^2)\widetilde{B}_{z1} = 0.\end{aligned} \tag{13}$$

- The component of the vertical of momentum equation

$$\begin{aligned}&(i\widetilde{k}_r\widetilde{\upsilon}_{r0} + i\widetilde{k}_z\widetilde{\upsilon}_{z0} - i\widetilde{\omega})\widetilde{\upsilon}_{z1} + (i\widetilde{k}_z\widetilde{m}^2)\widetilde{P}_1 + (i\widetilde{k}_z F)\widetilde{\psi}_{T1} + (i\widetilde{k}_z f_1\widetilde{\upsilon}_A^2)\widetilde{B}_{r1} +\\ &(i\widetilde{k}_z f_2\widetilde{\upsilon}_A^2)\widetilde{B}_{\phi 1} - (i\widetilde{k}_r f_1\widetilde{\upsilon}_A^2)\widetilde{B}_{z1} = 0.\end{aligned} \tag{14}$$

- The components of induction equations

$$f_1\widetilde{\upsilon}_{r1} + (\widetilde{\upsilon}_{r0} - i\widetilde{\omega})\widetilde{B}_{z1} - (i\widetilde{\omega} + i\widetilde{D}\widetilde{m}\epsilon\widetilde{k}_z)\widetilde{B}_{r1} - \widetilde{m}\epsilon\widetilde{B}_{\phi 1} = 0. \tag{15}$$

$$\gamma n(3 + n)\widetilde{B}_{r1} + 2(\widetilde{D}\widetilde{m}\epsilon\widetilde{k}_z^2 + i\widetilde{\omega})\widetilde{B}_{\phi 1} + 2i\widetilde{k}_r f_2\widetilde{\Omega}_1 = 0. \tag{16}$$

- Maxwell equation

$$(1 + i\widetilde{k}_r)\widetilde{B}_{r1} + i\widetilde{k}_z\widetilde{B}_{z1} = 0. \tag{17}$$

- Poisson equation

$$(i\widetilde{k}_r - \widetilde{k}_r^2 - \widetilde{k}_z^2)\widetilde{\psi}_{T1} - A\widetilde{\rho}_1 = 0. \tag{18}$$

- The state equation

$$\widetilde{P}_1 - \bar{\beta}_1\widetilde{\rho}_1 - (\bar{\beta}_1 + 4\bar{\beta}_2)\widetilde{T}_1 = 0. \tag{19}$$

- The energy equation

$$(\frac{\widetilde{m}^{\,2}}{\Gamma_3 - 1}(-i\widetilde{\omega}) + \frac{\widetilde{m}^{\,2}}{\Gamma_3 - 1}\widetilde{\upsilon}_{r0}(i\widetilde{k}_r))\widetilde{P}_1 + (-\frac{9\widetilde{D}\widetilde{m}\epsilon}{4} - \frac{7\widetilde{D}\widetilde{m}\epsilon n^2\gamma^2}{4} + \frac{\Gamma_1}{\Gamma_3 - 1}\widetilde{m}^{\,2}(i\widetilde{\omega}) - \frac{\Gamma_1}{\Gamma_3 - 1}\widetilde{m}^{\,2}\widetilde{\upsilon}_{z0}(i\widetilde{k}_z) - \frac{\Gamma_1}{\Gamma_3 - 1}\widetilde{m}^2\widetilde{\upsilon}_{r0}(i\widetilde{k}_r))\widetilde{\rho}_1 + (3i\widetilde{k}_r\widetilde{D}\widetilde{m}\epsilon + i\widetilde{k}_r\widetilde{D}\widetilde{m}\epsilon n\gamma)\widetilde{\Omega}_1 + 2f_2\widetilde{\upsilon}_A^{\,2}\widetilde{D}\widetilde{m}\epsilon(1 + i\widetilde{k}_r)\widetilde{B}_{\phi 1} + \bar{\beta}_2\widetilde{c}\widetilde{m}^{\,2}(i\widetilde{k}_r - \widetilde{k}_r^{\,2} + i\widetilde{k}_z - \widetilde{k}_z^{\,2})\widetilde{T}_1 = 0, \tag{20}$$

where dimensional variables and parameters are defined

$$\begin{array}{llll}
\widetilde{\rho}_1 = \dfrac{\rho_1}{\rho_0}, & \widetilde{P}_1 = \dfrac{P_1}{P_0}, & \widetilde{\psi}_{T1} = \dfrac{\psi_{T1}}{\psi_{T0}} & \\
\widetilde{T}_1 = \dfrac{T_1}{T_0}, & \widetilde{\Omega}_1 = \dfrac{\Omega_1}{\Omega_k}, & \widetilde{\Omega}_0 = \dfrac{\Omega_0}{\Omega_k} & \\
\widetilde{\upsilon}_{r1} = \dfrac{\upsilon_{r1}}{r\Omega_k}, & \widetilde{\upsilon}_{z1} = \dfrac{\upsilon_{z1}}{r\Omega_k}, & \widetilde{B}_{r1} = \dfrac{B_{r1}}{B_0} & \\
\widetilde{B}_{\phi 1} = \dfrac{B_{\phi 1}}{B_0}, & \widetilde{B}_{z1} = \dfrac{B_{z1}}{B_0}, & \widetilde{\upsilon}_A = \dfrac{\upsilon_A}{r\Omega_k} & \\
\widetilde{\omega} = \dfrac{\omega}{\Omega_k}, & \widetilde{m} = \dfrac{c_s}{r\Omega_k}, & \widetilde{k}_r = rk_r, & \\
\widetilde{k}_z = rk_z, & \bar{\beta}_1 = \dfrac{P_{0gas}}{P_0}, & \bar{\beta}_2 = \dfrac{P_{0rad}}{P_0}, & \widetilde{c} = \dfrac{c}{r\Omega_k},
\end{array} \tag{21}$$

and $\upsilon_A = B_0/\sqrt{\mu_0\rho_0}$ is Alfven speed. Also, we assume that $B_0$ is amount of magnetic field in the disk equilibrium state that $B_{r0} = f_1B_0, B_{\phi 0} = f_2B_0, B_{z0} = f_3B_0$, thus

$$\sqrt{f_1^2 + f_2^2 + f_3^2} = 1,$$

and on the other hand, for a dipole-symmetry magnetic field we have, $f_3 > f_2 > f_1$. $\widetilde{D} = H/r$ is the ratio of thick to the disk radius that we have used from a typical model [37]. Meantime,$\gamma$ is the ratio of the mass of the disk inner edge to the central object mass [33]. The quantity $n$ defined by its relationship between the under-study radius and the disk inner radius, $r = nr_0$, in which can be a parameter for investigating instability in different regions of the disk. Also, $\widetilde{A} = 4\pi G\rho_0r^2/\psi_{T0}$ shows the ratio of the disk gravitational potential to the total gravitational potential, therefore it is as parameter for considering of the presence of self-gravity in system and $0 < \widetilde{A} < 1$. If $\widetilde{A} \longrightarrow 1$, then $\psi_{disk} \gg \psi_M$, if $\widetilde{A} \longrightarrow 0.5$, then $\psi_{disk} \approx \psi_M$ and also if $\widetilde{A} \longrightarrow 0$, then $\psi_{disk} \ll \psi_M$.

## 3.1 Dispersion relation and numerical results

In the following, by forming a system of dimensionless perturbation equations from the previous section, the relevant coefficients matrix is achieved. Then, by obtaining the determinants of this matrix and equating them to zero, we find a relation for dispersion equation in which the general form of is as follow

$$G_5\widetilde{\omega}^{\,5} + G_4\widetilde{\omega}^{\,4} + G_3\widetilde{\omega}^{\,3} + G_2\widetilde{\omega}^{\,2} + G_1\widetilde{\omega} + G_0 = 0 \tag{22}$$

where $G_i (i = 0..5)$ are the equation coefficients. Also, since the perturbations have components in both vertical and radial axes, we define the dimensionless wave numbers of these two axes as $\widetilde{k}_r = \widetilde{k}\cos(t)$ and $\widetilde{k}_z = \widetilde{k}\sin(t)$ , in which $\widetilde{k}$ is the dimensionless perturbation wave number. Based on localized perturbation condition, we have $\widetilde{k} \gg 2\pi$. Also, $t$ is the angle that $\widetilde{k}$ forms with the disc plane, and in this paper, we assumed $t = \frac{\pi}{4}$. we solved equation (23) numerically. This fifth-order equation will have five answers. But only those unstable answers are important. According to the exponential function that we selected for the perturbation section, the imaginary and the positive part of the solution will be considered.

At first, we investigated the system stability in the state of no self-gravity ($\widetilde{A} = 0$), it should be noted that for other required parameters of the model, have been adopted values similar to Karimzadeh et al. (2020). For various regions the results is shown in Figure 1. This figure illustrates that the disk is unstable in the inner region and by moving away from the central object, instability decreases and the system is approximately stable in the disk outer edges. Next, we did the solution in the presence of self-gravity ($\widetilde{A} = 0.5$). Figures 2,3 and 4 is plotted respectively for $n = 1.5$ ,$n = 5$ and $n = 10$. The consequences shows which in the presence of self-gravity not only the system is unstable in all regions, but also the number of instability increase. It is clear that unlike solving without self-gravity, in this case, the disk is unstable in all regions.

# 4 The effect of the wind cooling on stability

Since the outflows can remove most of the gravitational energy released in disk, therefore they can help system cooling and a term can be assigned for their presence in the energy equation [38]. We added $Q^-_{wind}$ to the right side of the equation (8) as

$$Q^-_{wind} = \frac{1}{2}(\eta_b + \eta_k f^2)\bar{K} r^{\zeta+2}\Omega_k^2, \tag{23}$$

where $\eta_b, \eta_k, f, \bar{K}$ and $\zeta$ are defined parameters (Habibi & Abbasi 2019). Hence, in the case the model total cooling can write as

$$Q^-_{tot} = Q^-_{rad} + Q^-_{wind}, \tag{24}$$

where if the ratio of the radiation cooling to the disk total cooling is displayed with $\widetilde{q}$, therefore we have

$$Q^-_{wind} = (1 - \widetilde{q})Q^-_{tot}, \tag{25}$$

it is necessary to mention that $\widetilde{q}$ depends on the physical variables or parameters, but for simplicity, we applied it as a free parameter. By adding this term to the energy equation, we investigate system instability in the presence of wind cooling. All the dimensionless perturbation equations are the same as the previous section, except for the energy equation, which has rewritten as

$$\begin{aligned}&(\frac{\widetilde{m}^{\,2}}{\Gamma_3 - 1}(-i\widetilde{\omega}) + \frac{\widetilde{m}^{\,2}}{\Gamma_3 - 1}\widetilde{v}_{r0}(i\widetilde{k}_r))\widetilde{P}_1 + (-\frac{9\widetilde{D}\widetilde{m}\epsilon}{4} - \frac{7\widetilde{D}\widetilde{m}\epsilon n^2\gamma^2}{4} + \frac{\Gamma_1}{\Gamma_3 - 1}\widetilde{m}^{\,2}(i\widetilde{\omega}) - \\ &\frac{\Gamma_1}{\Gamma_3 - 1}\widetilde{m}^{\,2}\widetilde{v}_{z0}(i\widetilde{k}_z) - \frac{\Gamma_1}{\Gamma_3 - 1}\widetilde{m}^2\widetilde{v}_{r0}(i\widetilde{k}_r))\widetilde{\rho}_1 + (3i\widetilde{k}_r\widetilde{D}\widetilde{m}\epsilon + i\widetilde{k}_r\widetilde{D}\widetilde{m}\epsilon n\gamma)\widetilde{\Omega}_1 + \\ &2f_2\widetilde{v}_A^{\,2}\widetilde{D}\widetilde{m}\epsilon(1 + i\widetilde{k}_r)\widetilde{B}_{\phi 1} + (2 - \widetilde{q})\bar{\beta}_2\widetilde{c}\widetilde{m}^{\,2}(i\widetilde{k}_r - \widetilde{k}_r^{\,2} + i\widetilde{k}_z - \widetilde{k}_z^{\,2})\widetilde{T}_1 = 0.\end{aligned} \tag{26}$$

The dispersion equation will obtain from the way similar to the previous section. Also here, by choosing appropriate values for the model parameters, we have numerically solved the dispersion equation. we know that most of mass loss occurs at the inner regions of the disc by outflow, and also according to Figure 1. in the case without self-gravity, the system had been more unstable in the regions near the central object . Thus, we considered the effect of wind cooling on the stability of this region in absence of self-gravity. Figure 5. shows the results of this investigation. As seen, the wind cooling is effective on the stability of inner regions of the disc, and by increasing the share of wind cooling , the system will become more stable.

To study the effects of wind cooling on the instabilities of a magnetized disc with outflow and in presence of self-gravity, we did numerical solution for different regions with assuming $\widetilde{q} = 0.5$ and $\widetilde{A} = 0.5$. The results are shown in Figure 6, Figure 7 and Figure 8. In the previous section, it was observed that in presence of self-gravity, instability exist in all regions of disc. In this section, although we found that wind cooling reduces the strength of the system instabilities, but it can quench only one instability, thus the system will remain unstable.

## 5 Summary and discussion

The study of instabilities in accretion discs has always concerned astrophysicists. Numerous studies have been conducted in this subject, but the stability problem of the magnetized accretion disc with outflows is still being debated .Therefore, investigating a more comprehensive model to achieve results that are consistent with the observations is necessary. In this paper, we studied the stability of a the model of self-gravitating, magnetized accretion disc, which has a dipole-symmetry magnetic field that is produced by an $\alpha\omega - nature$ dynamo and this magnetic field can emanate winds from the disc's surfaces. It should be noted that the stability analysis performed in this paper has advantages over previous researches on magnetized accretion discs with outflows. Such that a larger number of perturbation variables have been studied simultaneously in the accretion system, which shows the comprehensiveness of this research. On the other hand, we know some characteristics and quantities of the disc, such as density, temperature, values for magnetic field components, inflow speed, etc., will not be the same throughout the disc and will have different values depending on the radius. In our proposed model, it is possible to investigate the stability of the system in different regions, which allows appropriate value selection for the variables and parameters defined of disk. The results show that even without self-gravity, there is possibility of a kind of instability near the compact accretor and as outer edge of the disc is approached, this instability will be quench. This result confirms the work done by LPP94 and Campbell(2009), We can say that this behaviour results from the reduction of the inflow speed and wind mass-loss rate in the outer regions of the disc.

On the other hand, when self-gravity was added to the model, it was seen that the number of accretion disc instabilities had increased and the system had become more unstable. This solution was performed for three different regions on the disc and the results show that generally, in the presence of self-gravity, all regions of the disc will be unstable, and by moving the closer to the outer edge of the disc, the intensity of one of these instabilities increases. In all literature that studied the stability of accretion disks with magnetically driven winds(mentioned in the introduction) self-gravity were neglected. Thus, this result , in itself, is of rather little surprise that the number of instabilities increase, sine we can say that gravitational instability is probably added [39]. In our initial investigations, the effect of outflow on the stability of the system was considered by adding some terms in continuity and momentum equations. We know that outflows not only transports mass and angular momentum but also they are a sink for energy ejection from the accretion disks. Thus, they can also affect the energy equation. For this purpose, a term was added for the presence of winds to the cooling part of the energy equation and the effect of wind cooling on the system stability was investigated.

First, the effect of wind cooling on the stability of the regions close to the central object in absence self-gravity was investigated. Results showed that by increasing the share of wind cooling, the growth rate of instability decreases, and the system progresses to stability. Then, to observe the effect of wind-cooling on the instabilities of the model in the presence self-gravity, by selecting an average value for the wind cooling parameter in the system, its effects on different regions of the disc were investigated. Results have shown that wind cooling is only effective in reducing one of the instabilities, so the system will still be unstable in all regions. This result is in agreement with the work of Li & Begelman (2014) that showed the outflow can help to disk stability. In summary, by considering the wind cooling, a magnetized disc with outflows can be almost stable that this outcome is almost close results in KW96 and CO02, but such a model would be unstable in the presence of self-gravity.

Astrophysicists believe there is a possibility of planet formation in discs around young stellar objects. Indeed, the main method for understanding planet formation lies in study of the protoplanetary disks, although the properties of disks relate directly to the planets that may potentially form but in these disks, which are generally thin and magnetized, self-gravity is considered and outflows is seen. On the other hand, Protoplanetary discs (PPDs) are host a number of instabilities that may play role directly or indirectly in the process of planetesimal formation [40-45]. Summarizing all the results in this paper and a review of research on PPDs, we can say that our proposed model can be a desirable model for accretion disks around young stellar objects. Since, not only it can justify the existence of jets in these types of discs [33], but also the resulting instabilities in model can relate to the formation of masses and eventually the formation of planets. Full investigation of each of these instability modes requires more research that we can provide in the next works.

**Data Availability:** The data that support the findings of this study are available from the corresponding authors, upon reasonable request.

# References

[1] Blandford, R. D., & Payne, D. G. 1982, Monthly Notices of the Royal Astronomical Society, 199, 883.

[2] Cao, X., & Spruit, H. C. 2013, The Astrophysical Journal, 765, 149.

[3] Ruden, S. 2004, The Astrophysical Journal, 605, 880.

[4] Knigge, C. 1999, Monthly Notices of the Royal Astronomical Society, 309, 409.

[5] Blandford, R. D., & Begelman M. C. 1999, Monthly Notices of the Royal Astronomical Society, 303, L1.

[6] Abbassi, S., Ghanbari, J., & Ghasemnezhad M. 2010, Monthly Notices of the Royal Astronomical Society, 409, 1113.

[7] Shadmehri, M. 2009, Monthly Notices of the Royal Astronomical Society, 395, 877.

[8] Schurch, N. J., Done, C., & Proga D. 2009, The Astrophysical Journal, 694, 1.

[9] Xue, L. S. L., & Wang, J. 2005, The Astrophysical Journal, 623, 372.

[10] Hennebelle, P., & Teyssier, R. 2008, Astronomy and Astrophysics, 477, 25.

[11] Banerjee, R., Vazquez-Semadeni, E., Hennebelle, P., & Klessen R. S. 2009, Monthly Notices of the Royal Astronomical Society, 398, 1082.

[12] Li, S. L., & Begelman, M. C. 2014, The Astrophysical Journal, 786, 6.

[13] Sadowski, A. 2016, Monthly Notices of the Royal Astronomical Society, 462, 960.

[14] Pringle, J. E. 1976, Monthly Notices of the Royal Astronomical Society, 177, 65.

[15] Vietri, M., & Stella L. 1998, The Astrophysical Journal, 503, 350.

[16] Hsu, Ch. Y., & Lin, M. K. 2022, The Astrophysical Journal, 937, 55.

[17] Goedbloed, H., & Keppens, R. 2022, The Astrophysical Journal, 259, 65.

[18] Clarke, C., & Carswell, R. 2007, Principles of Astrophysical Fluid Dynamics. Cambridge Univ. Press. England.

[19] Balbus, S. A., & Hawley, J. F. 1991, Astrophysical Journal, 376, 214.

[20] Balbus, S., & Hawley, J. F. 1998, Reviews of Modern Physics, 70, 1.

[21] Goldman, I., & Wandel, A. 1995, Astrophysical Journal, 443, 187.

[22] Zhu, Y., & Narayan, R. 2013, Monthly Notices of the Royal Astronomical Society, 434, 2262.

[23] Zhu, Z., Hartmann, L., Nelson, R. P., & Gammie C. F. 2012, Astrophysical Journal, 476, 110.

[24] Donati, J. F., Jardine, M. M., Gregory, S. G., Bouvier, J., Dougados, C., & Mnard, F. 2009, EAS Publications Series, 39, 133.

[25] Lubow, S. H., Papaloizou, J. C. B., & Pringle, J. E. 1994, Monthly Notices of the Royal Astronomical Society, 268, 1010.

[26] Koenigl, A., & Wardle, M. 1996, Monthly Notices of the Royal Astronomical Society, 279, L61.

[27] Krasnopolsky, R., Li, Z. Y., & Blandford, R. 1999, The Astrophysical Journal, 526, 631.

[28] Campbell, C. G. 2001, Monthly Notices of the Royal Astronomical Society, 323, 211.

[29] Cao, X., & Spruit, H. C. 2002, Astronomy and Astrophysics, 385, 289

[30] Koenigl, A. 2004, The Astrophysical Journal, 617, 1267.

[31] Campbell C. G. 2009, Monthly Notices of the Royal Astronomical Society, 392, 271.

[32] Habibi, A., & Abbassi, S. 2019, The Astrophysical Journal, 887, 256.

[33] Karimzadeh, S., Khesali, A. R., & Khosravi, A. 2020, Monthly Notices of the Royal Astronomical Society, 493, 2101.

[34] Shakura, N. I., & Sunyaev, R. A. 1973, Astronomy and Astrophysics, 24, 337.

[35] Campbell, C. G. 1999, Monthly Notices of the Royal Astronomical Society, 310, 1175.

[36] Piran, T. 1978, Astrophysical Journal, 221, 652.

[37] Campbell, C. G. 2010, Monthly Notices of the Royal Astronomical Society, 401, 177.

[38] Misra, R., & Taam, R. 2001, The Astrophysical Journal, 553, 978.

[39] Duschl, W. J., & Britsch, M. 2006, The Astrophysical Journal, 653, 89.

[40] Lehmann, M., & Lin, M. 2023, Monthly Notices of the Royal Astronomical Society, 522, 5892.

[41] Lin, M., Hsu, Ch. 2022, The Astrophysical Journal, 926, 24.

[42] Wu, Y., Lithwick, Y. 2021, The Astrophysical Journal, 923, 123.

[43] Huang, J., & et al. 2023, The Astrophysical Journal, 943, 107.

[44] Forgan, D. H. 2019, Monthly Notices of the Royal Astronomical Society, 485, 4465.

[45] Raquel, S. 2009, Astrophysics and Space Science Proceedings Series, 611.

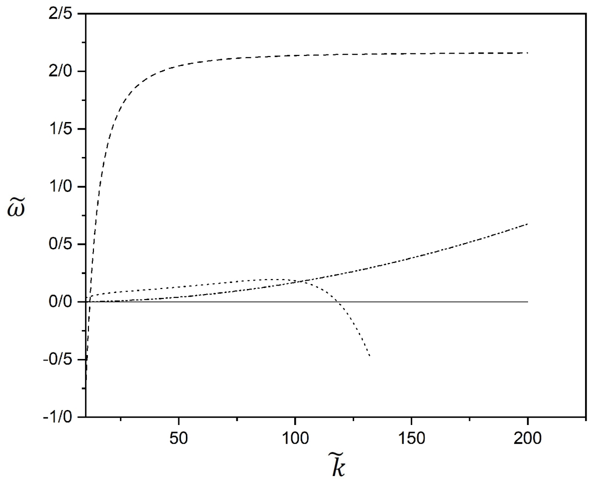


Figure 1: Investigation of model stability in the absence of self-gravity in different areas. Dash lines, dash-dot-dot lines and dot lines are for $n = 1.5$, $n = 5$, and $n = 10$ respectively.

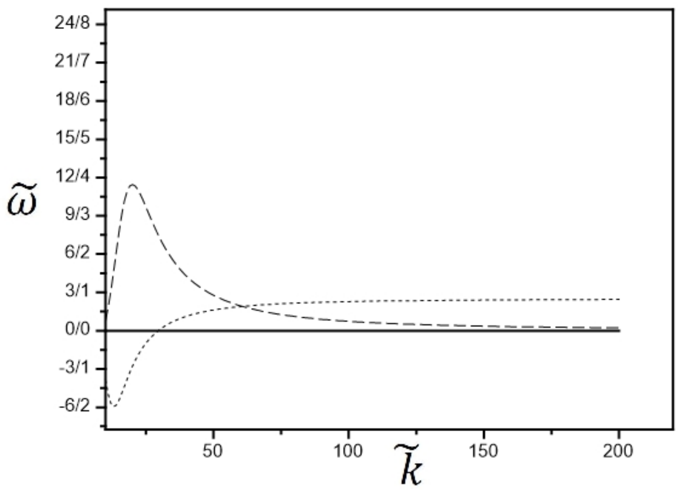


Figure 2: Investigation of model stability in the presence of self-gravity for $n = 1.5$, dash lines and dot lines display two instability in the model.

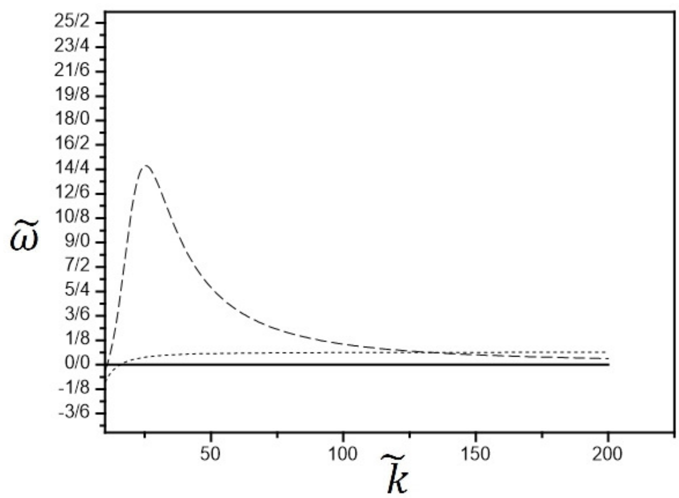


Figure 3: Investigation of model stability in the presence of self-gravity for $n = 5$, dash lines and dot lines display two instability in the model.

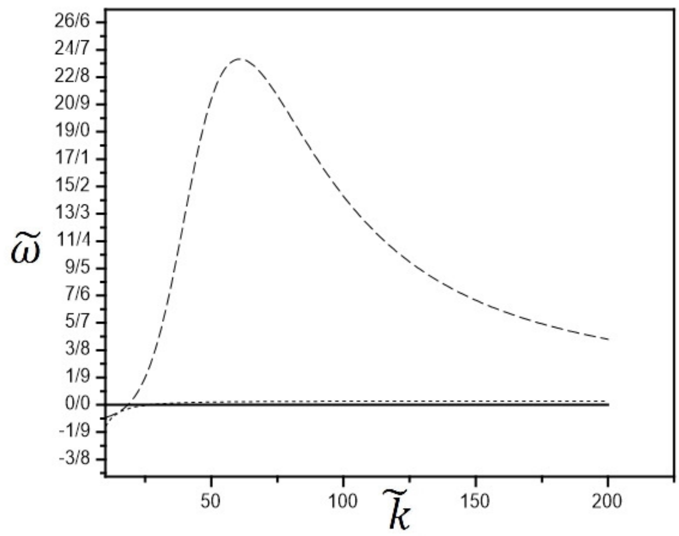


Figure 4: Investigation of model stability in the presence of self-gravity for $n = 10$, dash lines and dot lines display two instability in the model.

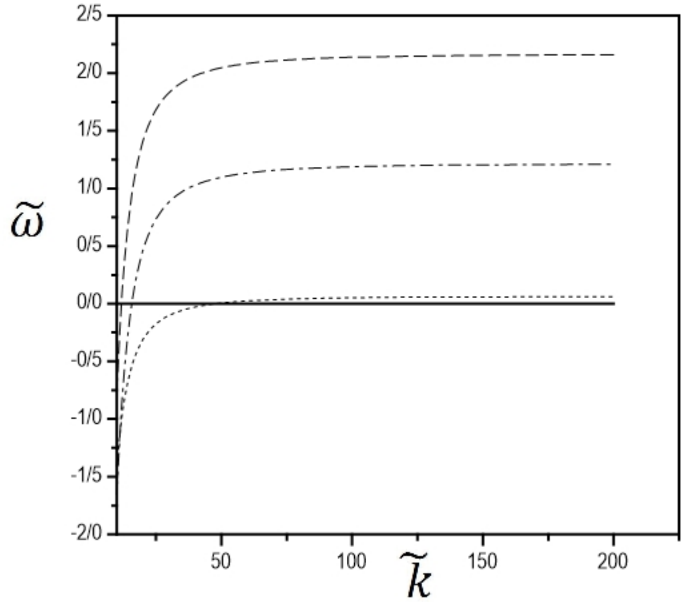


Figure 5: Investigation of model stability in the absence of self-gravity and in the presence of wind cooling for $n = 1.5$. Dash lines, dash-dot lines and dot lines are for $\widetilde{q} = 1$, $\widetilde{q} = 0.5$, $\widetilde{q} = 0.3$, respectively.

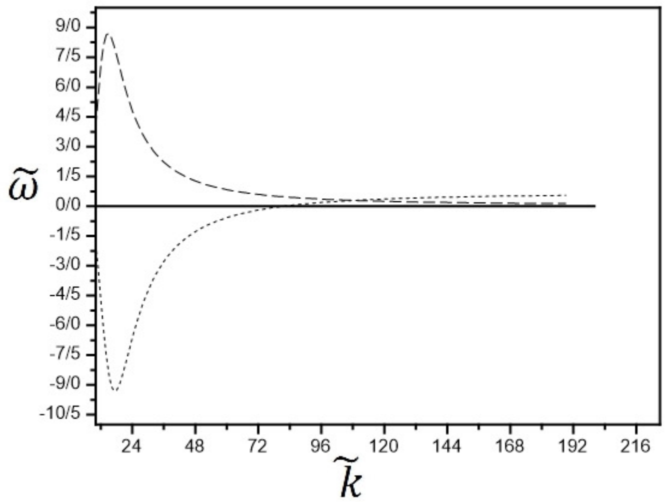


Figure 6: Investigation of model stability in the presence of self-gravity and wind cooling for $n = 1.5$.

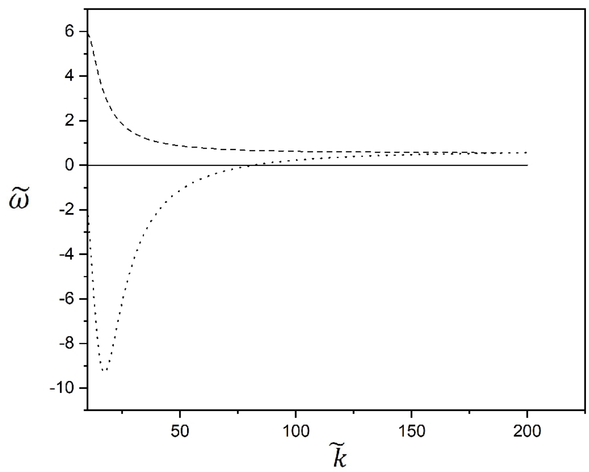


Figure 7: Investigation of model stability in the presence of self-gravity and wind cooling for $n = 5$.

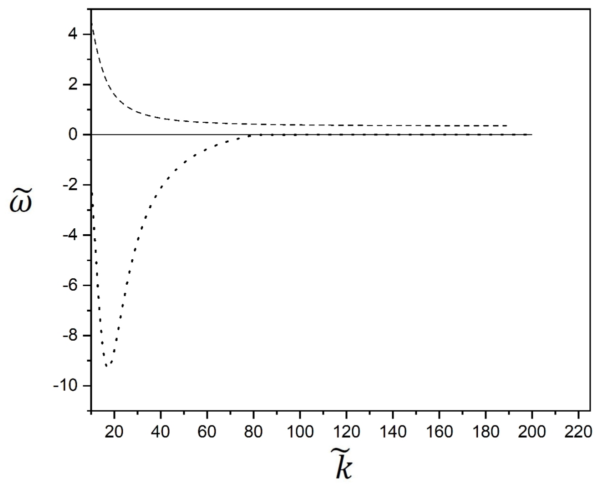


Figure 8: Investigation of model stability in the presence of self-gravity and wind cooling for $n = 10$.